Vol 17 No 3, March 2008
1674-1056/2008/17(03)/0865-13
Chinese Physics B
© 2008 Chin. Phys. Soc.
and IOP Publishing Ltd

Approximate entropy—a new statistic to quantify arc and welding process stability in short-circuiting gas metal arc welding*

Cao Biao(曹 彪), Xiang Yuan-Peng(向远鹏)†, Lü Xiao-Qing(吕小青),
Zeng Min(曾 敏), and Huang Shi-Sheng(黄石生)

College of Mechanical Engineering, South China University of Technology, Guangzhou 510641, *China*

(Received 15 December 2006; revised manuscript received 17 September 2007)

Based on the phase state reconstruction of welding current in short-circuiting gas metal arc welding using carbon dioxide as shielding gas, the approximate entropy of welding current as well as its standard deviation has been calculated and analysed to investigate their relation with the stability of electric arc and welding process. The extensive experimental and calculated results show that the approximate entropy of welding current is significantly and positively correlated with arc and welding process stability, whereas its standard deviation is correlated with them negatively. A larger approximate entropy and a smaller standard deviation imply a more stable arc and welding process, and vice versa. As a result, the approximate entropy of welding current promises well in assessing and quantifying the stability of electric arc and welding process in short-circuiting gas metal arc welding.

Keywords: approximate entropy, welding current, arc and welding process stability
PACC: 0547, 0650，0660V

1. Introduction

Quality monitoring and controlling in short-circuiting gas metal arc welding (GMAW-S) operation, especially electric arc and welding process stability analysis and evaluation, is an important factor in achieving higher productivity, lower cost and greater reliability of the welded components. A large number of scientific studies have been conducted to confirm the applicability of different arc signals to quality monitoring and controlling. Not only have various mechanisms been designed by which the welding signals are extracted from a particular physical process, but also different algorithms of signal analysis have been checked to assure the desired sensitivity and precision.

Kim and Eagar[1] disclosed the relationship between droplet sizes produced in gas metal arc welding (GMAW) and the stability of metal transfer. They found that droplet sizes predicted by using either the static force balance theory or the pinch instability theory played a key role in transiting metal transfer mode and arc stability. Sun and Wu[2] devised a special double-side arc welding setup, in which a plasma arc welding (PAW) and a tungsten inert gas (TIG) welding were connected in serial. They indicated that the PAW current was forced to flow through the keyhole along the thickness direction so as to compensate the energy consumed for melting the workpiece and hence weld penetration increased greatly. Some valuable analyses of arc and welding process instability phenomena in GMAW, which depend on arc length, the oxidizing potential of the shielding gas and the power supply output characteristic, were presented by Modenesi and Nixon.[3] It was found out that the instability process was associated with abrupt changes in arc current and voltage levels and could seriously affect operation by causing repulsive globular transfer in short-circuiting conditions. Hermans and Den[4] performed important investigations into the GMAW-S with the emphasis on process stability. The results showed that the welding process was the most stable when the short-circuiting frequency equalled the oscillation frequency of the weld pool. Kang and Rhee[5] developed a monitoring method by using different statistical parameters to access the welding process sta-

*Project supported by the National Natural Science Foundation of China (Grant Nos 50375053 and 50575077).
†Corresponding author. E-mail: xiangyp519@163.com

bility. Wu *et al*[6] devised an intelligent system for monitoring and recognition of process disturbances during GMAW-S, which was based on the measured and statistically processed data of welding electrical parameters. Grad *et al*[7] presented that the arc sound exhibited distinct characteristics for different welding situations and that from acoustic signals one could assess process stability and detect welding conditions resulting in weld defects. As a general rule, however, the aforementioned methods are either too complicated to be employed in practical applications or too susceptible to interferences to operate accurately.

GMAW-S using carbon dioxide (CO_2) as shielding gas features high efficiency, low energy consumption and low cost, and it finds a wide application in welding ferrous metals such as low-carbon steel and low-alloy steel. However, due to the arc instability with short-circuiting transfer, CO_2 GMAW-S has such drawbacks as high spatter and poor weld bead geometry. As a matter of fact, CO_2 GMAW-S process is a so much complicated phenomenon that its nonlinear nature, i.e. its chaotic state, has just been revealed quite recently.[8]

Generally speaking, in accordance with nonlinear dynamics theory, for purpose of studying a chaotic system, to calculate such characteristic parameters as Lyapunov exponent, correlation dimension, Kolmogorov entropy, etc, often requires a large number of data. Wolf *et al*[9] indicated that it required 10^m to 30^m points to fill out an m-dimensional strange attractor in the chaotic setting. In order to overcome this difficulty, in 1991 Pincus[10] put forward a concept of approximate entropy (ApEn), which immediately received much attention, academical and technological. The ApEn is such a novel statistic that it can be used as a measure to quantify the complexity or irregularity of both deterministic and stochastic signals. At present it has already been successfully applied to the analyses of chaotic pseudo-random sequence complexity,[11] heart rate variability,[12] endocrine hormone release pulsatility,[13] electroencephalographic (EEG) and cognition,[14] condition monitoring and fault diagnosis of mechanical equipment,[15] etc. The capability to discern changing complexity from a relatively small number of data and better outlier rejection ability show promise in application of ApEn to a large variety of engineering conditions.

Since the pioneering work of Lorenz in 1963, the nonlinear phenomena and chaos theory has attracted a great deal of attention in the engineering society, such as superconducting electronics,[16] tribology,[17] secure communications[18] and neural networks.[19] However, there are only few studies to our knowledge which focus on the electric arc and welding process stability from the viewpoint of chaos, especially the ApEn of welding current signals. Because of the nonlinear character of welding current signal, the ApEn can be used as a powerful tool in the study of CO_2 GMAW-S process. The present paper is mainly devoted to the problem of exploring arc and process stability in CO_2 GMAW-S by virtue of the chaotic parameter, ApEn. In particular, the goal of the paper is to attempt to propose a new numerical standard to accurately quantify and evaluate the arc and welding process stability in CO_2 GMAW-S.

2. The definition and algorithm of ApEn

For a better understanding of the ApEn, the definition of ApEn along with its computing procedure is described as follows.

Let the original data be $< x(n) >= x(1), x(2), \cdots, x(N)$, where N is the total number of data sequences. Two parameters must be fixed before ApEn can be computed, i.e.

m–embedding dimension of the vector to be formed,

r–a tolerance that functions as a noise filter.

(i) Form m-dimensional vectors $\boldsymbol{X}(1) - \boldsymbol{X}(N - m + 1)$ by defining

$$\begin{aligned} \boldsymbol{X}(i) =& [x(i), x(i+1), \cdots, x(i+m-1)], \\ i =& 1 - N - m + l. \end{aligned} \tag{1}$$

(ii) Define the distance between $\boldsymbol{X}(i)$ and $\boldsymbol{X}(j)$ (d[$\boldsymbol{X}(i)$, $\boldsymbol{X}(j)$]) as the maximum absolute difference between their corresponding scalar components, i.e.

$$\mathrm{d}[\mathbf{X}(i), \mathbf{X}(j)] = \max_{0 \le k \le m-1} [|x(i+k) - x(j+k)|]. \tag{2}$$

(iii) For a given $\boldsymbol{X}(i)$, based on a predefined value of r, calculate the value of $\mathrm{d}[\boldsymbol{X}(i),\ \boldsymbol{X}(j)]$ which is smaller than r, and then the ratio of the value to $N-m+1$, defined as $\mathrm{C}_i^m(r)$, namely

$$\mathrm{C}_i^m(r) = (N-m+1)^{-1} \times \sum_{j=1,j\neq i}^{N-m+1} \Theta(r - d[\mathbf{X}(i),\mathbf{X}(j)]), \qquad (3)$$

where $\Theta(\bullet)$ is Heaviside function.

(iv) Take the natural logarithm of each $\mathrm{C}_i^m(r)$, and average it over i, define $\Phi^m(r)$ as

$$\Phi^m(r) = (N-m+1)^{-1} \sum_{i=1}^{N-m+1} \ln \mathrm{C}_i^m(r). \qquad (4)$$

(v) Increase the dimension to m+l. Repeat steps (i)–(iv), and find $\mathrm{C}_i^{m+1}(r)$ and $\Phi^{m+1}(r)$.

(vi) In theory, ApEn is defined as

$$\mathrm{ApEn}(m,r) = \lim_{N\to\infty} [\Phi^m(r) - \Phi^{m+1}(r)]. \qquad (5)$$

In practice, the number of data points, N, is finite and the result obtained through the above steps is the estimate of ApEn when the data length is N, which can be denoted as

$$\mathrm{ApEn}(m,r,N) = \Phi^m(r) - \Phi^{m+1}(r). \qquad (6)$$

Obviously, the value of the estimate depends on m and r. As suggested by Pincus, m can be taken as 2 and r as (0.1–0.25) SD, where SD is the standard deviation from the original data sequence $< x(n) >$.

As a rule, in engineering practice, about 100 to 5000 data are needed to meet the requirements for estimating a robust value of ApEn. Consequently, in this paper the ApEn is calculated under the following conditions:

$$N = 5000, \quad m = 2, \quad \text{and} \quad r = 0.15\mathrm{SD}.$$

3. Analysis of the relationship between welding current ApEn and arc stability in CO_2 GMAW-S

In the present study the Fronius TPS2700 welding machine was used to conduct CO_2 gas shielded welding with short-circuiting transfer in 4 mm thick low carbon steel as bead on plate welds. H08Mn2SiA wire with a diameter of 1.0 mm was used as filler material and 99.9 vol% CO_2 as shielding gas.

At an electrode extension of 8mm, four groups of experiments were carried out with different process parameters, including wire feed rate (V_f), arc voltage (U_a), gas flow rate (V_q) and welding speed (V_w). In each group of welding experiments only one of the above-mentioned parameters was regulated to a series of typical values while the remaining three parameters were kept at some fixed values in order to study their individual influence separately. The welding current was real-time sampled for 50s by means of NI data acquisition card (DAQ PCI-6221) at a sample rate of 10000Hz. From the middle of total 50s of data samples , namely 12s, 120000 data points were extracted to calculate 24 welding current ApEn values corresponding to each different welding process parameter. (One ApEn value can be obtained from 5000 data.)

3.1. Effect of wire feed rate

Here, the CO_2 GMAW-S welding parameters are set at the values: 20V for arc voltage, 10 L/min for gas flow rate and 30cm/min for welding speed. The effects of wire feed rate were studied from 2.5 to 6.0m/min. The welding current waveform random in the first half a second and all the calculated ApEn values are shown in Figs.1 and 2, respectively. The mean value of all 24 ApEn, AV(ApEn), and standard deviation of ApEn, SD(ApEn), corresponding to each different wire feed rate are listed in Table 1 (The welding currents listed in Table 1 actually are mean values for all 12s sample data corresponding to each different parameter, so does the following.)

Comparative analysis of each different welding current waveform in Fig.1 shows that when wire feed rates are in the middle of testing range, i.e. at 4.0 and 4.5 m/min, the current waveforms are more regular and welding processes more uniform than those for other cases. When wire feed rate is beyond the range, it is clear that welding current waveforms are inclined to be erratic and inconsistent at some time. The analysis of current waveforms is presented as follows.

Obviously in an unstable welding process, first, the variation of metal droplet transfer period occurs, so the transfer frequency cannot keep constant. Next, the maximum value of short-circuiting welding current fluctuates considerably. More precisely, the standard deviation of the short-circuiting current is considerably large, which signifies the great fluctuation of arc and welding process. Finally, in the whole course of abnormal short-circuiting transfer, the time of arcing mismatches that of short circuit, or rather, the former is far longer than the latter. It means that too much energy accumulated during arcing directly results in too high short-circuiting current peaks and thus too many exploding spatters.

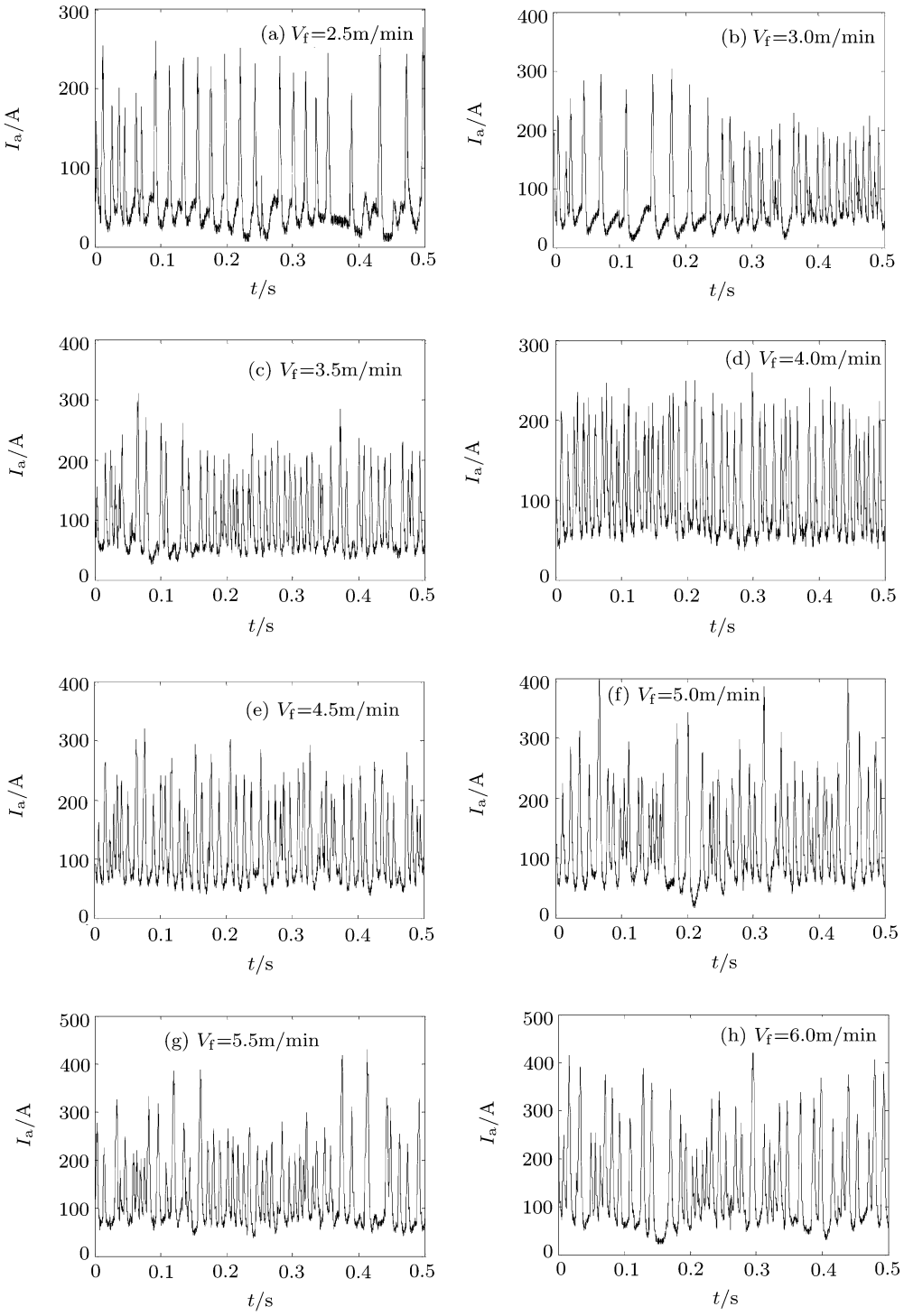


Fig.1. Welding current waveforms at different wire feed rates.

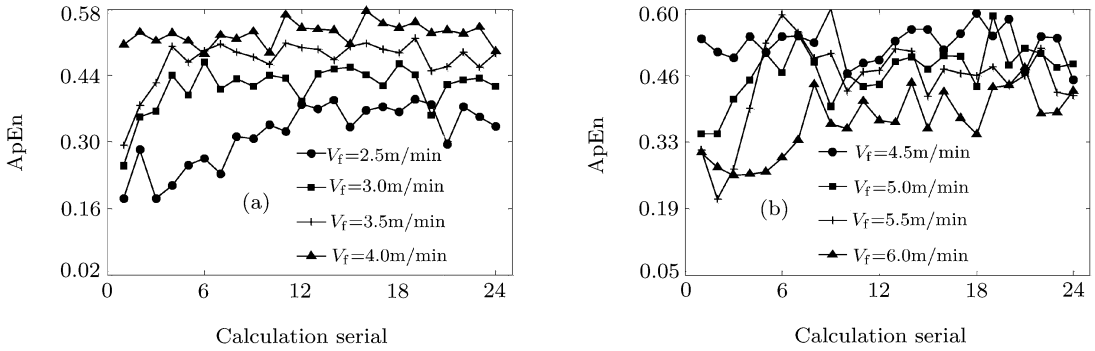


Fig.2. Values of ApEn at different wire feed rates.

Table 1. Welding current, AV(ApEn) and SD(ApEn) at different wire feed rates.

wire feed rate V_f/(m/min)	welding current I_a/A	AV(ApEn)	SD(ApEn)
2.5	66.3049	0.3160	0.0657
3.0	81.2489	0.4160	0.0474
3.5	94.0373	0.4724	0.0490
4.0	104.6464	0.5285	0.0230
4.5	115.2395	0.5295	0.0377
5.0	121.4839	0.4703	0.0561
5.5	128.6211	0.4517	0.0874
6.0	133.6843	0.3661	0.0668

When the wire feed rate is too slow, the welding current and welding current density are also small. The molten droplets are mainly subjected to the gravity force and surface tension. Only when they gradually conglomerate into a big liquid globule, which is too large for the surface tension to balance its gravity force, can they detach from the tip of wire and dip into the weld puddle. The constriction of CO_2 shielding gas causes the arc to contract, which leads to a high current density on the cathode spots. As a result, the molten droplets are subjected to a high repulsive force and thus reach a considerably unsteady state, which directly results in the wandering of arc or even a discontinuous weld seam.

In contrast, the high wire feed rate gives rise to a large short-circuiting current. Accordingly, the electromagnetic pinch force turns so high that it cannot only cause the droplets to detach dramatically from the tip of wire and impact the molten pool violently, but also constrict the short-circuiting liquid bridge between the filler end and the weld puddle heavily and try to end the short circuit in a time as short as possible. Meanwhile, because the wire feed rate exceeds the metal melting rate, the end of wire tends to submerge into the surface of the base metal, which often leads to the stubbing of the welding wire in the molten puddle, accompanied by highly irregular melt-off behaviour. At last it is unavoidable that the filler wire end bursts into pieces and thus high spatters are produced. Under these circumstances, the arc is surely unstable and welding process fluctuates greatly.

As illustrated in Fig.1, with wire feed rate increasing from 2.5 to 4.5m/min, the arc and welding process transition from an unsteady operation mode to a steady operation mode is observed. In view of the data presented in Table 1, the average value of ApEn of welding current, AV(ApEn), also increases from 0.3160 to 0.5295. However, while wire feed rate continues to increase from 4.5 to 6.0m/min, the welding process returns from a steady mode to an unsteady mode. The value of AV(ApEn) also drops from 0.5295 to 0.3661. Obviously, when the wire feed rate ranges from 4.0 to 4.5m/min, the values of AV(ApEn) reach maxima. From the above-mentioned, just under such circumstances, the arc and the welding process are the most stable of all. So it could be concluded that the more stable the arc and the welding process become, the larger the welding current ApEn will be. Further-

more, in accordance with the aforementioned definition and algorithm of ApEn, the ApEn is a measure of system complexity or irregularity. If the arc and the welding process are more steady, the fluctuation in welding current ApEn will be smaller, i.e. the standard deviation of ApEn, SD(ApEn) becomes smaller. The result is clearly shown in Fig.2. Numerical analyses of welding current AV(ApEn) and corresponding SD (ApEn) are illustrated in Fig.3. There is no doubt that when the arc and the welding process are the most stable at wire feed rates of 4.0 and 4.5m/min, the values of ApEn attain to maximal values and the values of SD(ApEn) reach minimal values in the experimental range.

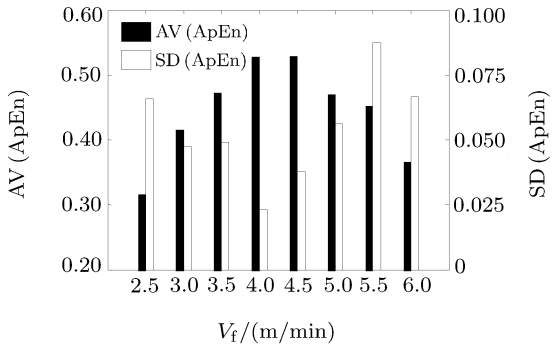


Fig.3. Effects of wire feed rate on welding current AV(ApEn) and its corresponding standard deviation SD(ApEn).

3.2. Effect of arc voltage

The experimental parameters are set at the values: 4.0m/min for wire feed rate, 10L/min for gas flow rate and 30cm/min for welding speed. The influence of arc voltage was investigated in a range from 14V to 26V. The welding current waveform random in the first half a second and all the calculated ApEn values are demonstrated in Figs.4 and 5, respectively. The values of welding current AV(ApEn) and its standard deviation SD(ApEn) corresponding to each different arc voltage are listed in Table 2.

Comparative analysis of each different welding current waveform in Fig.4 shows that when the arc voltage is at 20V, the electric arc and the short-circuiting transfer process are the most stable in the testing range. When the arc voltage is at other values except for 20V, it is obvious that welding current waveform turns nonuniform at intervals. The discussion about the current waveform analysis is the same as one that is detailed in Section 3.1. At low arc voltages, the short-circuiting liquid bridge between the filler wire end and the weld pool is not easy to break, which often causes the short-circuiting duration to be too long and the droplet transfer frequency to decrease. So the droplets dip into the weld puddle unevenly and stubbing of the filler wire in the weld pool starts to occur, accompanied by highly irregular melt-off behaviour, which leads to a lot of spatters and arc extinctions.

On the other hand, as a rule, a high arc voltage implies a long arc length. When the arc length is too long, i.e. it mismatches the welding current, the droplets at the tip of the filler wire gradually grow larger and larger, and subsequently swing about erratically. Quite often the droplets detach from the wire end and dip into the molten puddle in the direction not along but off the wire axis. In other words, the droplets fall into the weld pool in a free globular repelled mode instead of a short-circuiting transfer mode. Consequently, the incomplete fusion and high spatter are formed. Certainly, the arc and the welding process are unsteady.

According to the data presented in Table 2, it is evident that the arc voltage has a significant influence on the ApEn of welding current. As depicted in Fig.4, when the arc voltage is at 20V, the arc and the welding process are the most stable in the testing range. Just under such conditions, the value of AV(ApEn) is much larger than those at other arc voltages. This experimental result is in agreement with the fact that the appropriate arc voltage range for short-circuiting transfer is rather small, often between ±0.5V–1.5V. When the arc voltage increases from 14 to 20V, the arc and the welding process become more and more stable and also corresponding value of AV(ApEn) increases from 0.2988 to 0.5285. While the arc voltage continually increases from 20 to 26V, however, the welding process returns to an unsteady state and the value of AV(ApEn) decreases from 0.5285 to 0.2580 correspondingly. As shown above, it can be concluded that the more stable the arc and the welding process become, the larger the welding current ApEn will be. Moreover, as illustrated in Fig.5, the corresponding

fluctuation in ApEn, i.e. the value of SD(ApEn), is smaller. Numerical analyses of welding current AV(ApEn) and corresponding SD(ApEn) are illustrated in Fig.6. There is no doubt that the values of welding current AV(ApEn) attain to larger values and the values of their standard deviation SD(ApEn) reach smaller values when the welding process is relatively stable.

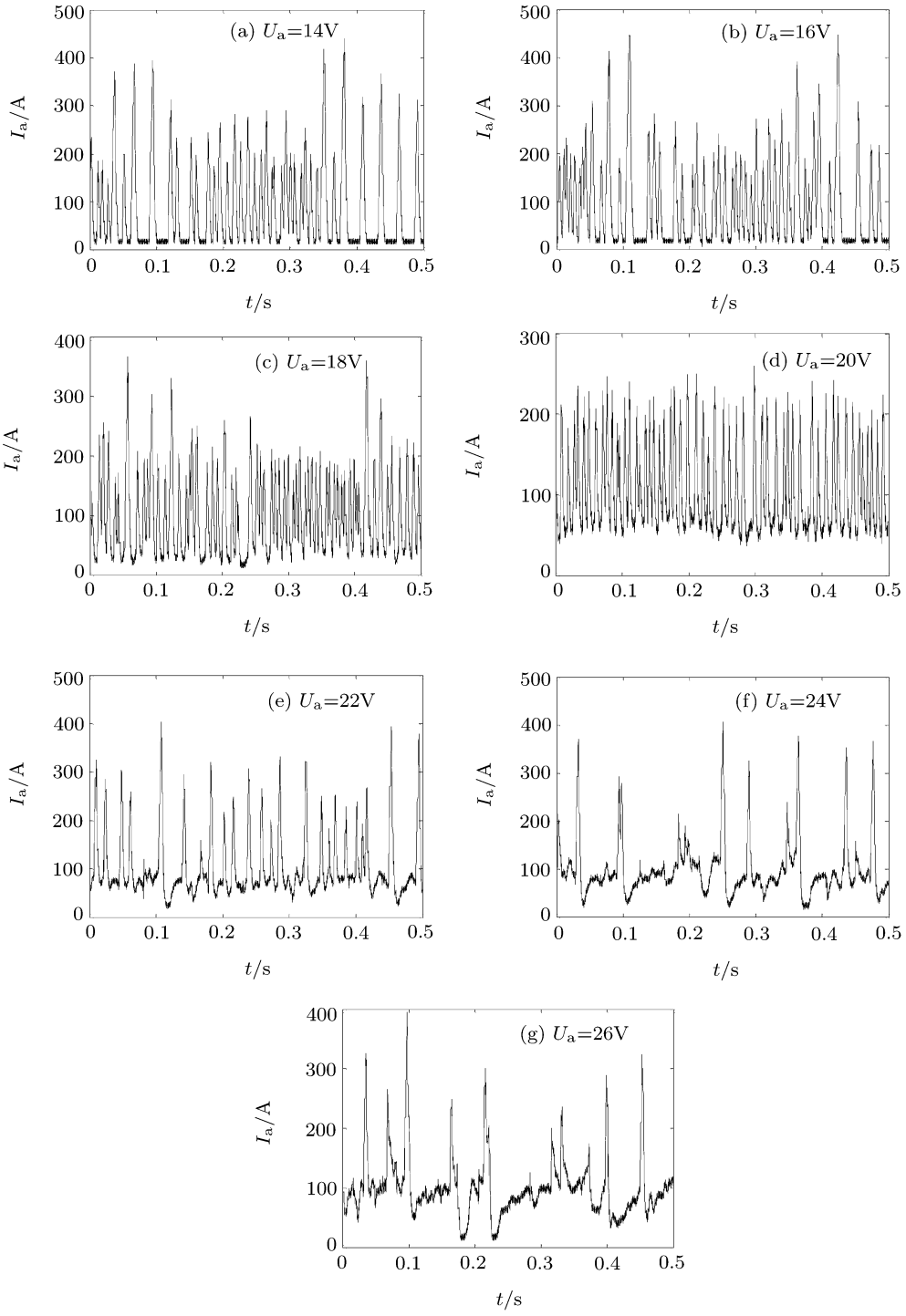


Fig.4. Welding current waveforms at different arc voltages.

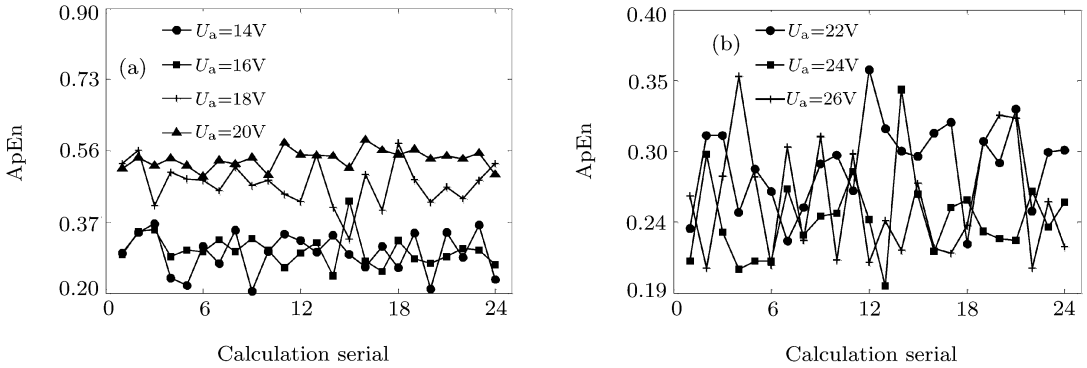


Fig.5. Values of ApEn at different arc voltages.

Table 2. Welding parameters, AV(ApEn) and SD(ApEn) at different arc voltages.

arc voltage U_a/V	welding current I_a/A	AV(ApEn)	SD(ApEn)
14	88.4165	0.2988	0.0512
16	89.9841	0.3050	0.0386
18	99.0989	0.4687	0.0533
20	104.6464	0.5285	0.0230
22	98.7526	0.2848	0.0320
24	97.3626	0.2453	0.0314
26	97.9708	0.2580	0.0427

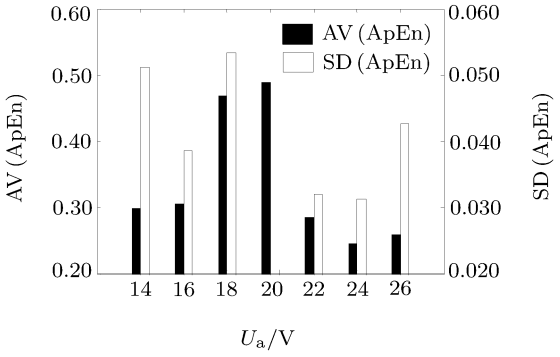


Fig.6. Effects of arc voltage on welding current AV(ApEn) and its corresponding standard deviation SD(ApEn).

3.3. Effect of gas flow rate

The welding parameters are set at the values: 4.0m/min for wire feed rate, 20V for arc voltage and 30cm/min for welding speed. The effect of gas flow rate is studied from 6 to 18L/min. The welding current waveform random in the first half a second and all the calculated ApEn values are demonstrated in Figs.7 and 8, respectively. The values of welding current AV(ApEn) and their standard deviation SD(ApEn) corresponding to each different gas flow rate are listed in Table 3.

Comparative analysis of each different welding current waveform in Fig.7 demonstrates that when gas flow rates are between 8 to 12L/min, the current waveforms are more regular and the welding processes are more uniform than those at other gas flow rates. Also the discussion about the current waveform analysis is the same as one that is detailed in Section 3.1. Too low a gas flow rate makes the stiffness of shielding gas stream insufficient to evacuate air from the weld zone and protect the transfer droplets and the molten puddle from being contaminated through oxidization.

On the contrary, too high a gas flow rate causes the shielding gas stream to impact on the weld pool violently and the molten metal to solidify too early to fill the weld pass. So the droplet spreadability and clearance fillability deteriorate. More severely, shielding gas turbulence starts to occur, which often convolves air into the weld zone unavoidably. Consequently, the weld seam is susceptible to porosity and high oxidation spatter is generated.

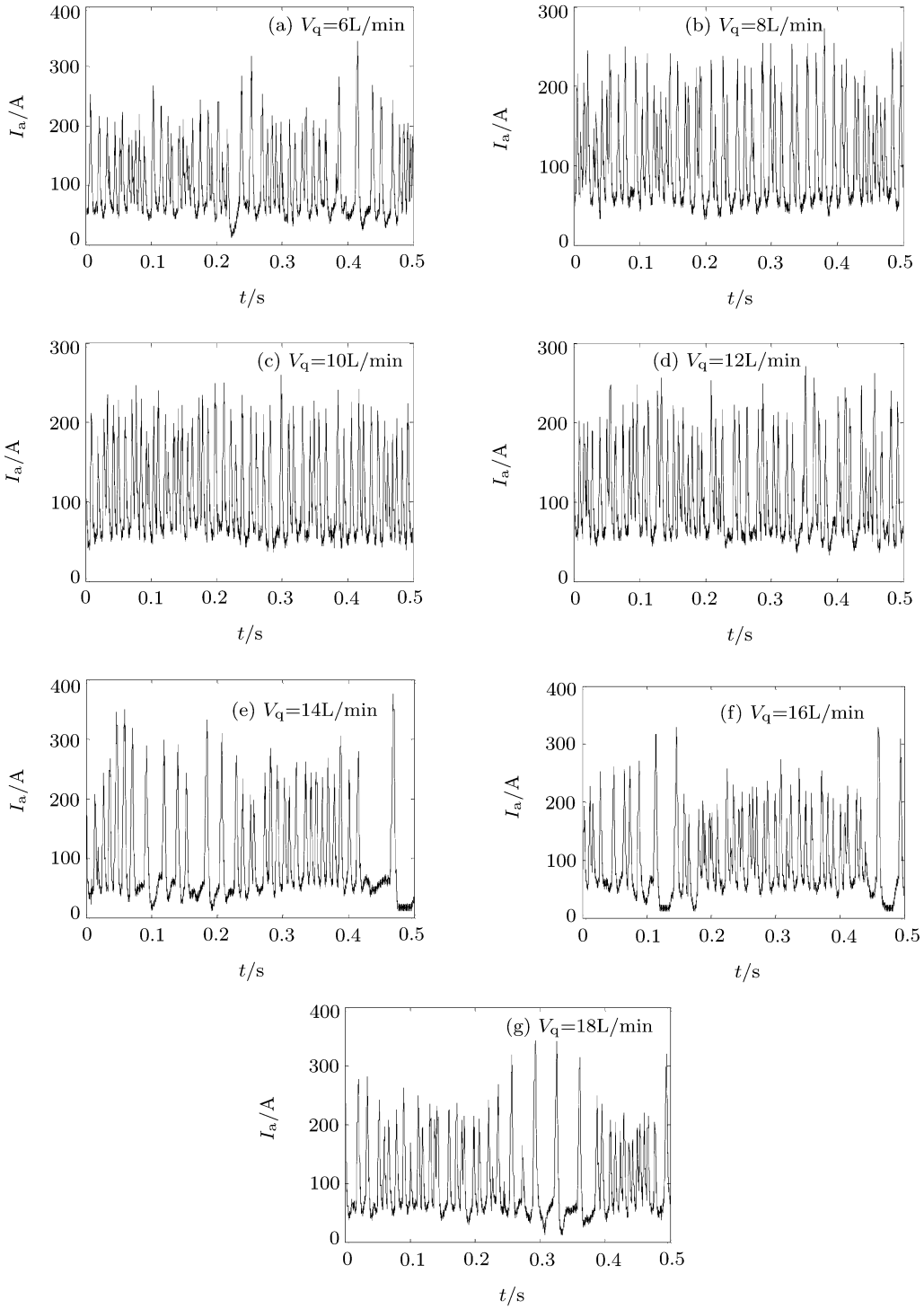


Fig.7. Welding current waveforms at different gas flow rates.

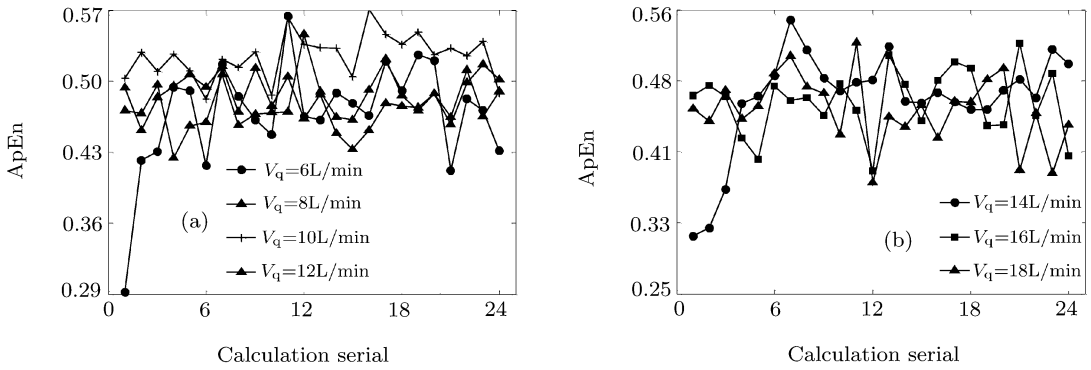


Fig.8. Values of ApEn at different gas flow rates.

Table 3. Welding current, AV(ApEn) and SD(ApEn) at different gas flow rates.

gas flow rate V_q/(L/min)	welding current I_a/A	AV(ApEn)	SD(ApEn)
6	101.9970	0.4699	0.0552
8	103.2626	0.4811	0.0263
10	104.6464	0.5285	0.0230
12	103.8901	0.4846	0.0237
14	102.6777	0.4629	0.0563
16	102.2911	0.4596	0.0360
18	102.1883	0.4510	0.0381

According to the data presented in Table 3, while the gas flow rates are between 8 and 12L/min, the values of AV(ApEn) are larger than those at other gas flow rates. What is more, as illustrated in Fig.8, the corresponding fluctuations in welding current ApEn, SD(ApEn) are also smaller. Obviously, just under these circumstances, the arc and the welding process are the most stable of all. So the same conclusion could be drawn that when the arc and the welding process become more stable, the welding current ApEn should be larger and SD(ApEn) smaller, which can be readily observed from numerical analyses of welding current AV(ApEn) and its corresponding standard deviation SD(ApEn) illustrated in Fig.9.

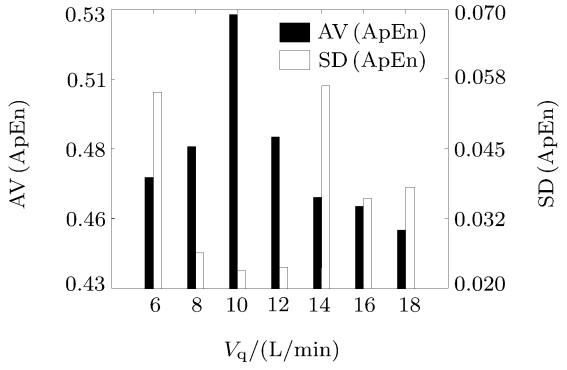


Fig.9. Effects of gas flow rate on welding current AV(ApEn) and its corresponding standard deviation SD(ApEn).

3.4. Effect of welding speed

The welding parameters are set at the values: 4.0m/min for wire feed rate, 20V for arc voltage and 10L/min for gas flow rate. The effect of welding speed is investigated in a range from 21 to 39cm/min. The welding current waveform random in the first half a second and all the calculated values of ApEn are depicted in Figs.10 and 11, respectively. The values of welding current AV(ApEn) and their standard deviation SD(ApEn) corresponding to each different welding speed are listed in Table 4.

Comparative analysis of each different welding current waveform in Fig.10 shows that when the welding speed is in the intermediate testing range, i.e. between 30 and 33cm/min, the current waveforms are more regular and the welding process is more uniform than those for other cases. When welding speed is beyond the range, it is clear that waveforms tend to be erratic and unevenly varied with time. The discussion

about the current waveform analysis is the same as one that is detailed in Section 3.1. While the welding speed is too low, the molten metal is inclined to flow to the front of the weld pass, which makes the CO_2 arc burn on the surface of the molten metal other than on the base metal surface. Consequently, a large amount of molten metal piles up rather than fully penetrates into the weld seam. The droplets dip into weld pool erratically, and the arc wandering directly results in the coarse weld morphology as well as the poor weld bead geometry.

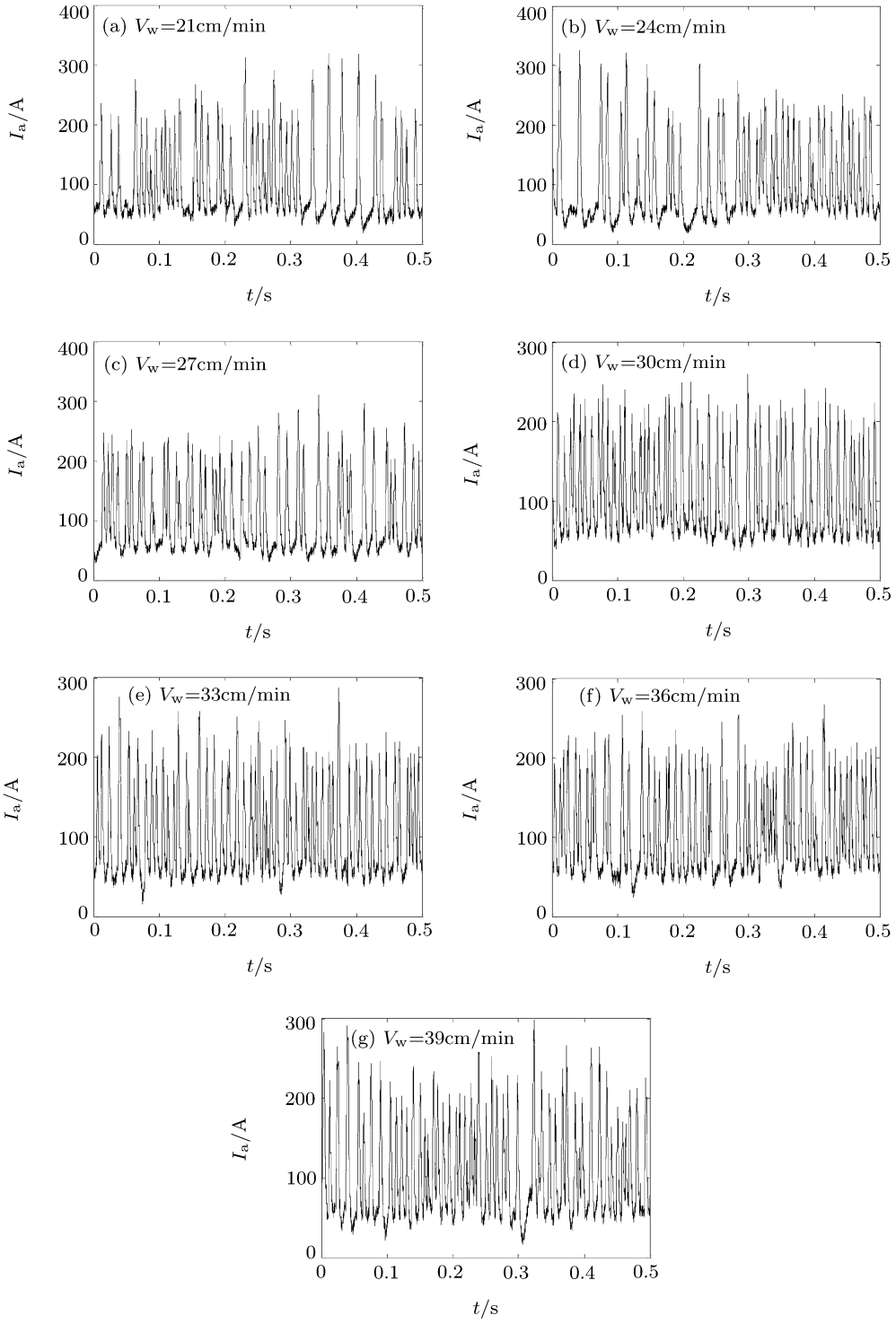


Fig.10. Welding current waveforms at different welding speeds.

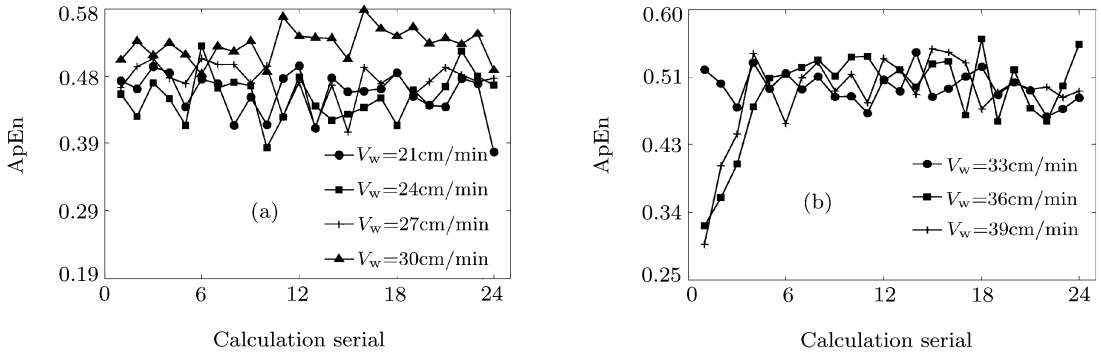


Fig.11. Values of ApEn at different welding speeds.

Table 4. Welding current, AV(ApEn) and SD(ApEn) at different welding speeds.

welding speed V_w/(cm/min)	welding current I_a/A	AV(ApEn)	SD(ApEn)
21	102.6806	0.4578	0.0310
24	101.9238	0.4528	0.0335
27	102.8420	0.4750	0.0279
30	104.6464	0.5285	0.0230
33	101.6106	0.4994	0.0208
36	102.4709	0.4922	0.0604
39	102.8620	0.4913	0.0546

On the contrary, with the increase of welding speed, the thermal energy per unit length of seam which the arc transfers to the base metal also increases owing to the arc burning on the surface of base metal directly. But with the further increase of welding speed, the transferred thermal energy per unit length of seam decreases. As a result, the base metal melts less and molten pool solidifies more rapidly, which often leads to undercut and bad weld shape. The reason is that in the case of high speed welding, there is insufficient molten metal to fill the arc travelling path and, additionally, the molten metal gathers toward the seam centre as a result of surface tension. Furthermore, the weld pool is too long to hold itself steady, which frequently gives rise to humped beads. The CO_2 arc wanders and welding process fluctuates. Only when the welding speed is in an appropriate range, which matches the welding current, can the droplets transfer smoothly and the weld be performed satisfactorily.

According to the data presented in Table 4, with the welding speed increasing from 21 to 30cm/min, the value of AV(ApEn) also increases from 0.4578 to 0.5285. However, while the welding speed continues to increase to 39 cm/min, the value of AV(ApEn) drops from 0.5285 to 0.4913. Obviously, when the welding speeds are between 30 and 33cm/min, the values of AV(ApEn) reaches maximal values. What is more, as illustrated in Fig.11, the corresponding fluctuations in welding current ApEn, SD(ApEn), reach minimal values. From the above-mentioned, just under such conditions, the arc and the welding process are the most stable of all. Again, the same results can be obtained that when arc and process become more stable, the value of welding current ApEn will be larger, and the value of SD(ApEn) smaller. It can be seen clearly from the numerical analyses of welding current AV(ApEn) and corresponding SD(ApEn) shown in Fig.12.

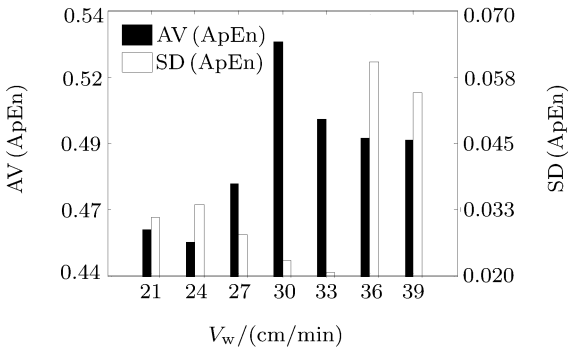


Fig.12. Effects of welding speed on welding current AV(ApEn) and its corresponding standard deviation SD(ApEn).

4. Conclusion

In this paper, we have investigated the relationship of welding current ApEn with the stability of electric arc and welding process from the viewpoint of nonlinearity and chaos. More accurately, using the property of ApEn which can give the robust estimate from short data and is attractive to dynamic analysis, we have shown that the welding current ApEn and its standard deviation SD(ApEn) are significantly correlated with the arc and the welding process stabilities. More specifically, when the arc and the welding process transit from an unstable operation mode to a stable operation mode by regulating different process parameters including wire feed rate, arc voltage, gas flow rate and welding speed, the values of welding current ApEn turns larger and the value of SD(ApEn) smaller correspondingly. What is more, the more stable the arc and the welding process become, the larger value the ApEn reaches and the smaller value the SD(ApEn) attains to. Additionally, the reverse is true for the variation trends of the values of ApEn and SD(ApEn) when the arc and the process stabilities deteriorate.

To sum up, the ApEn has huge potential utility to analyse the arc and the welding process stabilities in GMAW-S due to its salient features. It can be concluded that the larger value the welding current ApEn reaches and the smaller one the SD(ApEn) attains, the more stable the arc and the welding process will be. So the welding current ApEn gives large opportunities for the quantifying and monitoring of the arc and the welding process stabilities in GMAW-S.

References

[1] Kim Y S and Eagar T W 1993 *Weld. J.* **72** 269

[2] Sun J S and Wu C S 2002 *Acta Phys. Sin.* **51** 286 (in Chinese)

[3] Modenesi P J and Nixon J H 1994 *Weld. J.* **73** 219

[4] Hermans M J M and Den O G 1999 *Weld. J.* **78** 137

[5] Kang M J and Rhee S 2001 *Weld. J.* **80** 1

[6] Wu C S, Hu Q X, Sun J S, Polte T and Rehfeldt D 2004 *Proc. the Institution of Mechanical Engineers* Part B *J. Engng. Manufacture* **218** 1145

[7] Grad L, Grum J, Polajnar I and Slabe J M 2004 *Int. J. Machine Tools and Manufacture* **44**(Amsterdam: Elsevier) 555

[8] Lü X Q, Cao B, Zeng M and Huang S S 2005 *Transactions of the China Welding Institution* **26** 65 (in Chinese)

[9] Wolf A, Swift J B, Swinney H L and Vastano J A 1985 *Physica* D **16** 285

[10] Pincus S M 1991 *Proc. the National Academy Sciences USA* **88** 2297

[11] Cai J P, Li Z and Song W T 2003 *Acta Phys. Sin.* **52** 1871 (in Chinese)

[12] Pincus S M and Goldberger A L 1994 *Am. J. Physiol.* **266** H1643

[13] Pincus S M, Mulligan T, Iranmanesh A, Gheorghiu S, Godschalk M and Veldhuis J D 1996 *Proc. the National Academy of Sciences USA* **93** 14100

[14] Xie Y, Xu J X, Yang H J and Hu S J 2002 *Acta Phys. Sin.* **51** 205 (in Chinese)

[15] Xu Y G, Li L J and He Z J 2002 *Inform. Contr.* **31** 547 (in Chinese)

[16] Du H C, Liao H Y and Zhou S P 2003 *Chin. Phys.* **12** 557

[17] Yuan X P, Chen H B and Zheng Z G 2006 *Chin. Phys.* **15** 1464

[18] Huang X G, Yu P and Huang W 2006 *Chin. Phys.* **15** 2894

[19] Wang M S, Hou Z H and Xin H W 2006 *Chin. Phys.* **15** 2553